The Onset of Flow-induced Vibrations in a Square Tube Array subjected to Cross-Flow

YEHIA KHULIEF, SAIF AL-KAABI, SAID SEID and MUHAMMAD ANIS
Department of Mechanical Engineering
King Fahd University of Petroleum & Minerals
KFUPM Box 1767, Dhahran 31261
SAUDI ARABIA
khulief@kfupm.edu.sa; www.kfupm.edu.sa/me/khulief/htm

Abstract:- The need for accurate prediction of vibration and wear of heat exchangers in service has placed greater emphasis on improved modeling of the associated phenomenon of flow-induced vibrations. It was recognized that modeling of the complex dynamics of fluidelastic forces, that give rise to vibrations of tube bundles, requires a great deal of experimental insight. Accordingly, the prediction of the flow-induced vibration due to unsteady cross-flow can be greatly aided by semi-analytical models, in which some coefficients are determined experimentally. In this paper, the elastodynamic model of the tube array is formulated using the finite element approach, wherein each tube is modeled by a set of finite tube-elements. The interaction between tubes in the bundle is represented by fluidelastic coupling forces, which are defined in terms of the multi-degree-of-freedom elastodynamic behavior of each tube in the bundle. A laboratory test rig with an instrumented square bundle is constructed to measure the fluidelastic coefficients used to tune the developed dynamic model. The test rig admits two different test bundles; namely the inline-square and 45^{o} rotated-square tube arrays. Measurements were conducted to identify the flow-induced dynamic coefficients. The developed scheme was utilized in predicting the onset of flow-induced vibrations, and results were examined in the light of TEMA predictions. The comparison demonstrated that TEMA guidelines are more conservative in the two configurations considered.

Keywords:- Flow-induced Vibrations, Heat Exchangers, Tube Bundles, Cross Flow

1. Introduction

Pressure fluctuations around heat exchanger tubes result in fluid-structure dynamic coupling, which give rise to vibrations in all tubes of the bundle. To gain more insight into this phenomenon, researchers resorted to dynamic modeling of such systems. However, modeling the dynamics of fluidelastic motions due to crossflow over a tube bundle is too complicated to be investigated only analytically. At present, there is no such a reliable analytical model that accurately describes the phenomena of flow-induced vibration over a bank of tubes. Accordingly, a reliable mathematical model requires some tuning via experimental measurements.

The flow-induced vibration phenomena of tube bundle vibrations caused by shell-side flow in heat exchangers were addressed early in the literature, Wallis [1] and Putnam [2]. Today, the literature in the area of research has become very rich with a large number of publications addressing these problems and suggesting different methods of predictions and solutions. These include approximate analytical models, analytical models with purely structural emphasis, semi-analytical models where modeling simplifications were attributed to complementary experimental investigations, and pure experimental studies dedicated to understanding and identification of such excitation mechanisms. Progress in research activities related to this problem was reviewed by Paidoussis [3], Price [4], and Weaver et al. [5]. In addition, some books were dedicated to present a rather detailed account of this problem; e.g. the books by Chen [6], and Katinas and Zukauskas [7].

A number of theoretical investigations have been conducted on flow-induced vibrations in heat exchangers. Chen [8, 9], in his sequel papers, presented a general theoretical approach to characterizing the instability mechanisms of a group of tubes in crossflow. Cai et al. [10] reported a theoretical investigation of the fluidelastic instability of loosely supported tubes in non-uniform crossflow, wherein the unsteady flow theory was employed. Their instability analysis, however, was restricted to the inactive phase of tube motion. Further investigations were suggested to study the instability mechanism during the active mode of tube motion. Eisinger et al. [11] applied a numerical model to simulate the fluidelastic vibration of a representative tubes in a tube bundle based on unsteady flow theory. The numerical simulation was performed using the general purpose ABAQUS-EPGEN finite element code using a special subroutine incorporating fluidelastic forces. An analytical computational fluid dynamics technique was introduced by Ichioka et al. [12] to study fluidelastic vibration of tube bundles in heat exchangers. The technique was based on the moving mesh method which was developed by the authors. Kassera and Strohmeier [13] introduced a two-dimensional simulation model for the flow induced vibrations in tube bundles. The flow field equations including turbulence were solved using the boundary element method; however the tubes were structurally treated as rigid cylinders supported by linear elastic strings. Fischer and Strohmeier [14] introduced a coupled fluid-structure interaction model to evaluate stability of tube bundles in cross-flow. A three-dimensional transient model is developed, which was augmented by a structural response model based on beam theory and frictional impact.

It has become evident that modeling of the complex dynamics of fluidelastic forces that give rise to vibrations of tube bundles requires a great deal of experimental insight. Experimental investigations of the phenomenon of flow-induced vibrations in heat exchangers was recognized and pursued for the following two reasons: (a) to gain more insight into the nature of such complex dynamic behavior, and (b) to reduce the complexity of the derived mathematical models in the light of some experimental findings. Grover and Weaver [15, 16] presented a sequel of experimental studies of cross flow-induced vibration of tube array, and pointed out some observations over the range of their tests. Based on experimental results, they concluded that only a single elastic tube and the flow streams immediately adjacent to either side of the tube are required to model the essential features of the fluidelastic system. To account for some fluid elastic effects that could not be tackled by the quasi-steady flow theory, Tanaka et al. [17-19], introduced a method for calculating the critical flow velocity based on the unsteady flow theory. Equations were presented in matrix form including coupling, and experimental measurements were utilized to determine the fluid-induced force coefficients. Granger [20] used the same linear model of the fluidelastic forces by Chen [8] to write the dynamic model for a tube bundle in crossflow. Experimental measurements were performed on a tube bundle with several instrumented tubes, and the measured modal parameters were then used to determine the global damping and natural frequency, which in turn used to determine the fluidelastic force coefficients. A methodology for modeling flow-induced vibrations of tubes in crossflow was presented by Chen et al. [21, 22]. The unsteady flow theory is utilized in establishing the fluidelastic force coefficients. The fluid-force coefficients were stated analytically and justified by experiential measurements. They concluded that fluidelastic coefficients depend on tube arrangement, pitch, oscillation amplitude, reduced flow velocities, and Reynolds number.

Although a considerable progress has been made in the area of flow-induced vibrations since the early seventies, it remains necessary to understand the flow-induced vibration mechanisms for all possible flow situations. To date, there are no accurate criteria by which one could pinpoint the onset of fluidelastic instability in heat exchangers. The criteria set by TEMA [23] are relied upon in industry, though it is not adequate in predicting the onset of damaging flow-induced vibrations in many situations.

In this paper, a fluidelastic dynamic model using the finite element approach is developed for a square tube bundle in crossflow. The resulting nonlinear dynamic model admits the unsteady fluidelastic coupling in terms of experimentally measured force coefficients. Once such coefficients are experimentally determined, they are inserted into the generalized non-self-adjoint eigenvalue problem. The resulting nonlinear eigenvalue problem is iteratively solved and the instability conditions, referring to the onset of vibrations, are determined.

2. The elastodynamic model

Based on the actual heat exchanger construction, all the tubes of the tube bundle are normally made of the same material and having same cross-sectional dimensions. The developed formulation, however, is written in a general form to admit different geometrical and material properties for each elastic component. The following are the basic assumptions underlying the elastodynamic modeling: (a) the material of the elastic tube is homogeneous and isotropic; (b) the deflection of the tube is produced by the displacement of points of the centerline; and (c) the shear deformation for such slender tube configuration is neglected. Now, let us consider an element of the elastic tube for which the nodal coordinates are defined by $\{q\}$. Using the Lagrangean approach, we can write the equations of motion of tube i as

$$[M^i]\{\ddot{q}_i\}+[D^i]\{\dot{q}_i\}+[K^i]\{q_i\}=\{Q_i\} \quad (1)$$

The finite element expressions of the coefficient matrices are given by

$$\begin{aligned}[K] &= \int_0^l [B_e]^T EI[B_e]dx \\ &+ \int_0^l [B_a]^T EA[B_a]dx \\ &+ \int_0^l [B_\varphi]^T GJ[B_\varphi]dx\end{aligned} \quad (2)$$

and

$$\begin{aligned}[M] &= \int_0^l [N_v]^T \rho_s A[N_v]dx \\ &+ \int_0^l [N_\theta]^T I\ [N_\theta]dx \\ &+ \int_0^l [N_\varphi]^T I_p[N_\varphi]dx\end{aligned} \quad (3)$$

where $\{Q_i\}$ is the generalized force vector that may contain all externally applied forces, and may also contain the time-dependent fluidelastic coupling forces, $[D^i]$ is the damping matrix, $[B_e]=\partial[N_\theta]/\partial x$, $[B_a]=\partial[N_t]/\partial x$ and $[B_\varphi]=\partial[N_\varphi]/\partial x$ are the derivatives of the shape function matrices $[N_\theta]$, $[N_t]$, and $[N_\varphi]$, respectively, as given by Perzemieniecki [24], or Bazoune et al. [25].

The dynamic equations of motion that represent the elastodynamic behavior of the tube can be derived using the Lagrangean approach. Denoting $\{q_i\}$ as the vector of nodal displacements of tube i, one can substitute the Lagrangean function in the variational form, carry out the associated differentiations, and then perform standard finite element assembly procedure to express the equation of motion of tube i in the following final form:

$$[M^i]\{\ddot{q}_i\}+[D^i]\{\dot{q}_i\}+[K^i]\{q_i\}=\{Q_i\} \quad (4)$$

The fluid-structure interaction, as manifested by the fluidelastic forces can be represented to include the coupling between the adjacent tubes in the tube bundle. Let the fluidelastic force that couples tube i and tube j be

$$F_{ij}=C_{D_{ij}}\dot{s}_{ij}+C_{K_{ij}}s_{ij} \quad (5)$$

where s_{ij} is a vector in the *yz*-plane, which represents the distance between tube i and tube j, $C_{D_{ij}}$ is the damping coefficient that depends on the tube diameter, fluid density and the bundle gap velocity. $C_{K_{ij}}$ is the stiffness coefficient that depends on the fluid density and the bundle gap velocity. Using the virtual work expression, one can write the work done by F_{ij} as

$$\begin{aligned}\delta W_{F_{ij}} &= -F_{ij}\ \ \delta s_{ij}-F_{ij}[\partial s_{ij}/\partial q_i]\ \ \delta q_i \\ &\quad -F_{ij}[\partial s_{ij}/\partial q_j]\ \ \delta q_j \\ &= Q_F^{iT}\ \ \delta q_i\ +\ Q_F^{jT}\ \ \delta q_j\end{aligned} \quad (6)$$

The vectors Q_F^i and Q_F^j are the generalized forces associated with the fluidelastic coupling between tube i and tube j. These forces are to be added to the right hand side of the equation of motion. For the rest of the derivation, the subscript s is introduced to refer to the intrinsic structural properties, e.g. structural mass, damping and stiffness properties, while the subscript f refers to the corresponding fluidelastic terms. Now, equation (4) can be written for tubes i and j, including the added-mass effect, as

$$\begin{aligned}&\begin{bmatrix} M^i & 0 \\ 0 & M^j \end{bmatrix}\begin{Bmatrix} \ddot{q}_i \\ \ddot{q}_j \end{Bmatrix}+\begin{bmatrix} D_s^i & 0 \\ 0 & D_s^j \end{bmatrix}\begin{Bmatrix} \dot{q}_i \\ \dot{q}_j \end{Bmatrix} \\ &+\begin{bmatrix} K_s^i & 0 \\ 0 & K_s^j \end{bmatrix}\begin{Bmatrix} q_i \\ q_j \end{Bmatrix}=\begin{Bmatrix} Q_F^i \\ Q_F^j \end{Bmatrix}\end{aligned} \quad (7)$$

where M is the mass matrix that includes both the structural inertia properties and the added-mass effects., i.e. $M^i = M_s^i + M_f^i$. The added-mass matrix M_f^i is a function fluid density and the tube dimensions. Equation (7) can be written in a general assembled form to represent all active tubes in the tube array. The added-mass effects as well as the coupling fluidelastic forces are determined experimentally by estimating the fluidelastic coefficients.

3. The fluidelastic forces

The linearity assumption of the fluid-dynamic forces has been verified by some experimental investigators, e.g. Tanaka et al. [19], and consequently the superposition principle can be applied to express the fluidelastic forces. Accordingly, the total force acting on the center tube (*O*) is obtained by the superposition of the fluidelastic forces due to the vibration of the individual tubes (each one of the tubes *O*, *L*, *R*, *U* or *H*) when the rest of the tubes are stationary. Therefore, the fluid-dynamic forces (per unit length) on the center tube (*O*) in *y*- and *z*-directions can be expressed as follows:

$$F_Y = \frac{1}{2}\rho_f V_g^2 \left\{ \begin{array}{l} C_{YOY} Y_O + C_{YLY}(Y_L + Y_R) \\ + C_{YLZ}(Z_L - Z_R) \\ + C_{YUY} Y_U + C_{YDY} Y_D \end{array} \right\} \quad (8)$$

$$F_Z = \frac{1}{2}\rho_f V_g^2 \left\{ \begin{array}{l} C_{ZOZ} Z_O + C_{ZLY}(Y_L - Y_R) \\ + C_{ZLZ}(Z_L + Z_R) \\ + C_{ZUZ} Z_U + C_{ZDZ} Y_D \end{array} \right\} \quad (9)$$

where C_{YLZ}, etc., are fluid-dynamic coefficients, as explained in [26]. Each coefficient is identified by three suffixes. The first suffix indicates the direction of the fluid force, the second indicates the position of the vibrating tube, and the third suffix indicates the direction of tube vibration.

The dependence of the mass matrix on the natural frequency results in a nonlinear eigenvalue problem. Neumaier [27] presented an inverse iteration scheme for the nonlinear eigenvalue problem. A class of nonlinear eigenvalue problems encountered in solid-structure problems has been addressed by Conca et al. [28]. The scheme adopted in this paper employs an inverse iteration outer loop with the MATLAB complex eigenvalue solver as its inner core. The method first calculates structural stiffness, mass and damping matrices for the tube bundle. It also interpolates the fluid force coefficients by curve fitting so that these coefficients can be determined at any iteration step of the reduced velocity. It then updates the stiffness, mass and damping matrices with the current value of fluidelastic effects. The modal characteristics of the whole system (tube bundle) are then determined by solving the associated complex eigenvalue problem. The critical reduced velocity is defined as the reduced velocity at the onset of instability. The iteration is indexed over the reduced velocity, and the iteration is terminated once the critical reduced velocity is reached. In other words, the critical reduced velocity is one at which the highest real part of an eigenvalue change its sign from negative (stable region) to positive (unstable region).

4. The experimental setup

To simulate the flow-induced vibration in tube bundles, an experimental water loop was designed and built for this study. The water loop is a closed type loop, which consists of a water circulation tank, a primary 30-HP water pump (in conjunction with a secondary 20 HP water pump), a 3-m^3 (3000 Liter) head tank and a damping tank. The experimental setup used in this investigation is shown in Figure 1. The water is pumped from the lower circulation tank into the upper head tank. The controlled flow of water passes through a damping tank, which houses a series of screens, and then into the rectangular test channel. Two control valves control the flow velocity and water level in the channel.

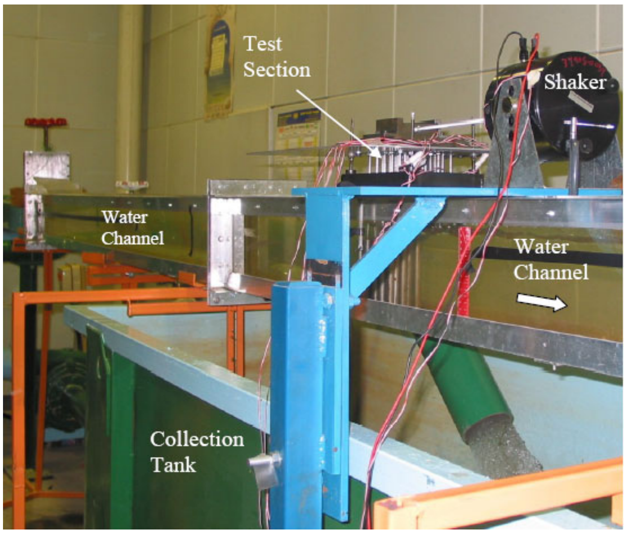

Figure 1: The experimental test rig

The test rig admits two different test bundles; namely the inline-square and 45^o rotated-square tube arrays, as shown in Figures 2 and 3, respectively. The test section carries the tube bundle that consists of 25 tubes; with 1.45 pitch-to-diameter ratio for square and 2.0 for rotated square arrays, [29]. The shaker is used to excite the center tube (tube *O*) in *x*- and *y*-direction at a range of frequencies. The experimental tube bundle is shown in Figure 4. The tube is made of steel with 1.85-cm (0.725-in) diameter and 12-cm (4.72-in) length. The tube is supported by a flexible thin steel cylinder of 0.5-cm (0.2-in) diameter and15-cm (5.9-in) length. All other tubes are identical. Due to symmetry, only four active tubes (tubes *O*, *L*, *U*, and *H*) are instrumented; each with two strain gages. One strain gage is mounted along the flow direction (*z*- or 0^o- direction) and the other strain gage is mounted along the perpendicular direction to the flow (*y*- or 90^o-direction). Only the active lengths of the test tubes are submerged with water at any time. All tubes, except for the center one, are clamped to a heavy steel support plate.

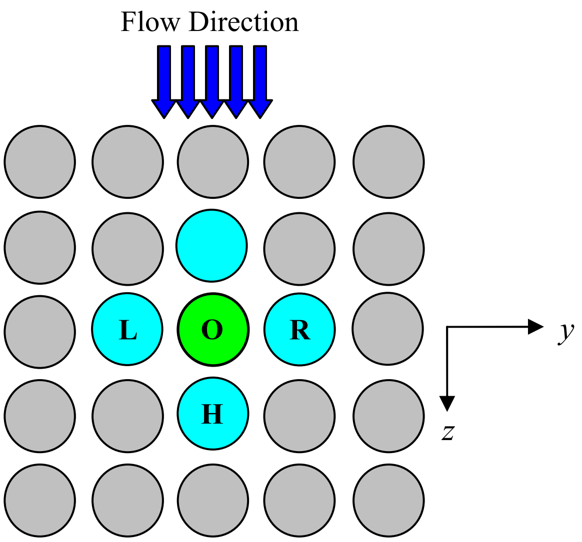

Figure 2: The inline square tube array (Pitch-to-diameter ratio of 1.45)

Figure 4 shows the instrumented test section. The exciter control (Brüel & Kjær type 1047) is used to generate an excitation sinusoidal signal with a selected excitation frequency. This signal is then amplified using a power amplifier (Brüel & Kjær type 2718) before it is fed to the shaker. The response signals of the strain gages are captured and processed by the multi-channel scanner (***Vishay*** Model 6100). The scanner is controlled via a PC loaded with ***StrainSmart™*** 6000 software. Strain gages used to measure forces were calibrated by the static method.

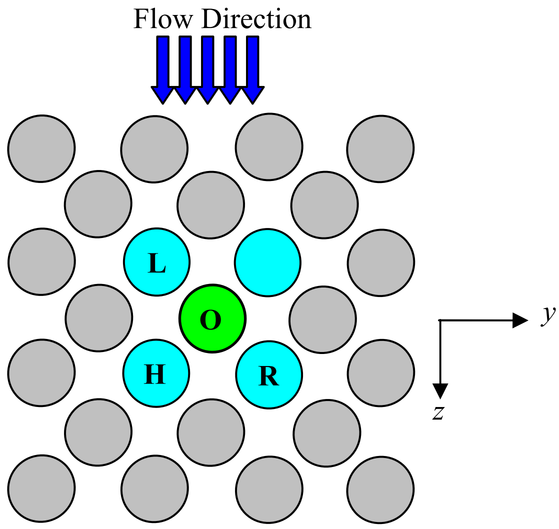

Figure 3: The rotated square tube array (Pitch-to-diameter ratio of 2.0)

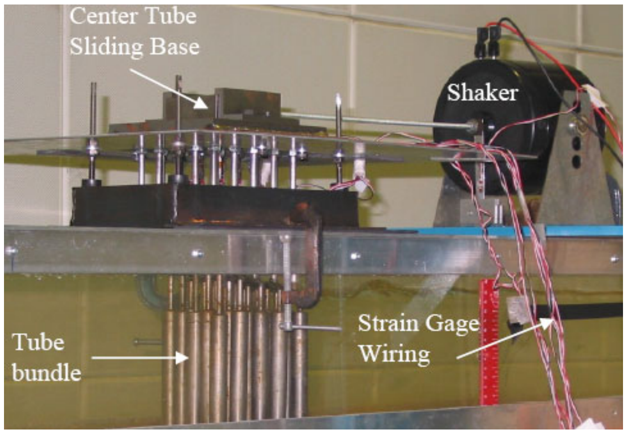

Figure 4: The instrumented test section

5. Data acquisition and analysis

The data acquisition sessions included the recording of measurements of nine strain gages at the following permuted settings:

1. The shaker frequency is varied within the range 1-18 Hz, with several increments.
2. The shaker position is varied between (a) flow direction ($\theta = 0$) and (b) perpendicular to flow direction ($\theta = 90^o$); and step (1) is repeated in each case.
3. Steps (1) and (2) are repeated for several values of flow velocities, staring from zero velocity (still water), in addition to one measurement in air.

Upon processing the acquired data, one could identify phase difference, and the fluidelastic

ISSN: 1790-5117

ISBN: 978-960-474-185-4

mass, damping, and stiffness coefficients needed for the computational algorithm.

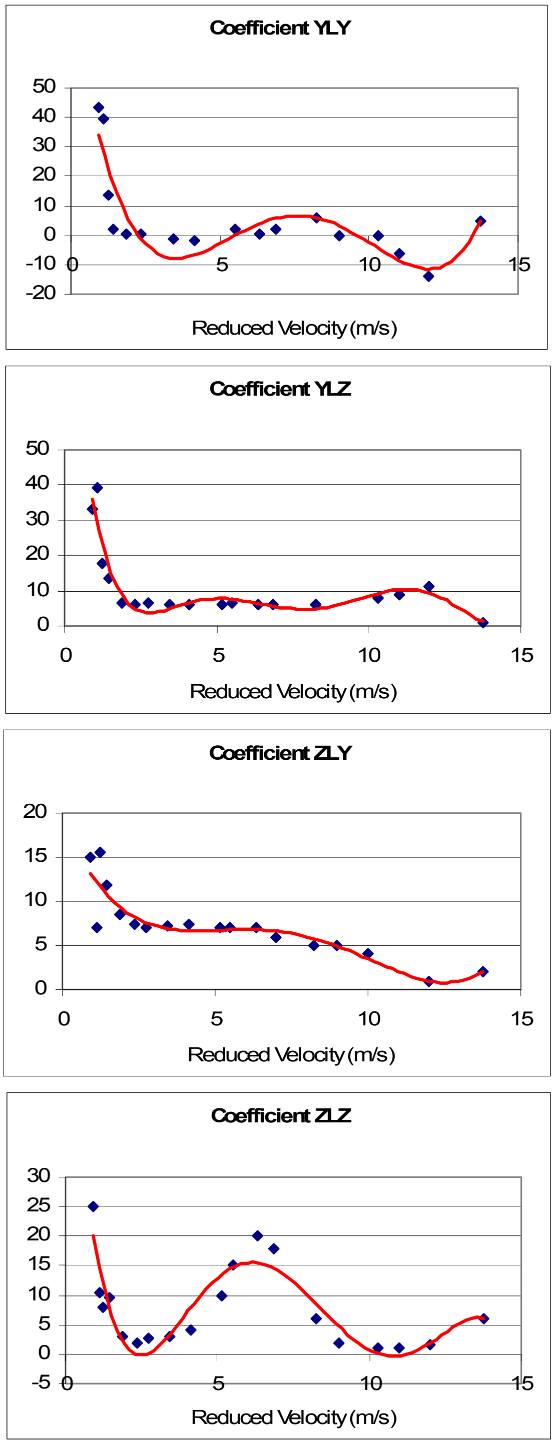

Figure 5: Amplitude of fluid-force coefficient for in-line square array

In order to proceed with experimental analysis, one needs to measure the natural frequencies of the tube in air and in water through dynamic damping tests. The following values were found from those measurements: the damping

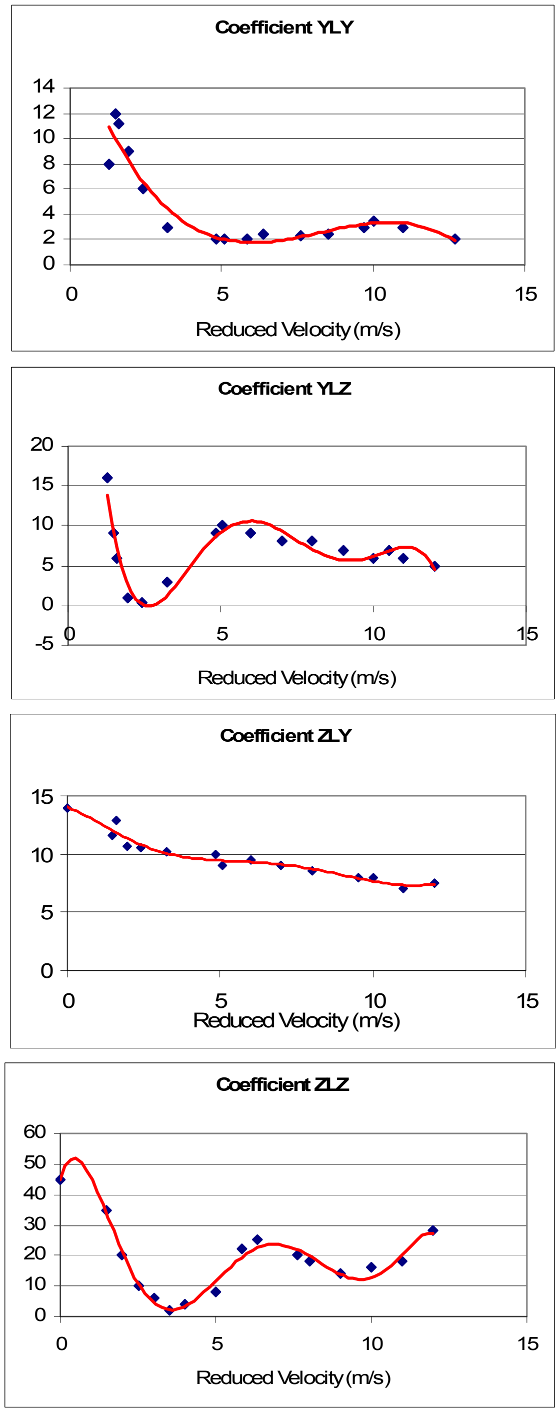

Figure 6: Amplitude of fluid-force coefficient for rotated square array

factors are $\zeta = 0.0144$ in air and $\zeta = 0.0344$ in water, while the corresponding fundamental frequencies are found to be $f_n = 20.25\,\text{Hz}$ in air and $f_n = 18.99\,\text{Hz}$ in water.

Measurements and processing of data resulted in the fluidelastic coefficients, as manifested by the added mass coefficients, as well as the fluid elastic force coefficients; both magnitude and phase. Figures 5 and 6 display the fluidelastic force coefficient of both inline-square and rotated-square acting on tube *L,* respectively. Similarly, the complete set of fluidelastic coefficients is identified for further utilization of the numerical prediction scheme. It is noteworthy to note the phase difference between the tube vibrations and the fluid dynamic forces; wherein a positive phase difference indicates that the force is leading the tube displacement. It was also observed that change of sign of the phase difference corresponds to the fluid dynamic force switching from a damping force to an exciting force. Similar behavior was also observed by previous investigators [17], and was attributed to the possible contribution of the Karman vortex or similar vortices at lower velocities.

The developed prediction scheme was then tested in comparison to TEMA standards. The TEMA guidelines for estimating the critical flow velocity for the onset of tube bundle vibrations are given in the **Standards of Tubular Exchanger Manufacturers Association**, Mechanical Standards, Class RCB, Section 5, [23]. The critical velocity estimate v_c is given by

$$v_c = \frac{\Gamma f_n d_o}{12} ft/\sec \qquad (10)$$

where

$\Gamma \equiv$ *Dimensionless critical flow Velocity parameter*
$f_n \equiv$ *Fundamental natural frequncy* $(c/\sec)$
$d_o \equiv$ *Outside diameter of tube* $(inches)$

The dimensionless parameter Γ is given for different tube array configurations as a function of tube pitch, effective weight of tube per unit length, and the logarithmic decrement. For the two cases tested in this investigation; inline square and rotated-square tube arrays, the estimates produced by our computational scheme, which are based on the experimentally evaluated fluidelastic coefficients, were compared to that obtained using the above TEMA empirical formulas, Figures 7 and 8. The comparison shows that TEMA estimates are in the conservative side. In addition, one notes that the estimate predicted by TEMA's formula is less sensitive to tube pitch variations.

6. Conclusions

The Elastodynamic model of the tube array is formulated using the finite element approach, wherein each tube is modeled by a set of finite tube-elements. The interaction between tubes in the bundle is represented by fluidelastic coupling forces, which are defined in terms of the

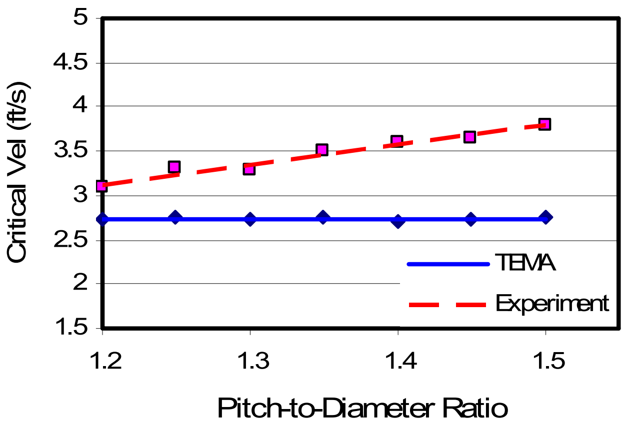

Figure 7: Critical velocity estimates for inline square array

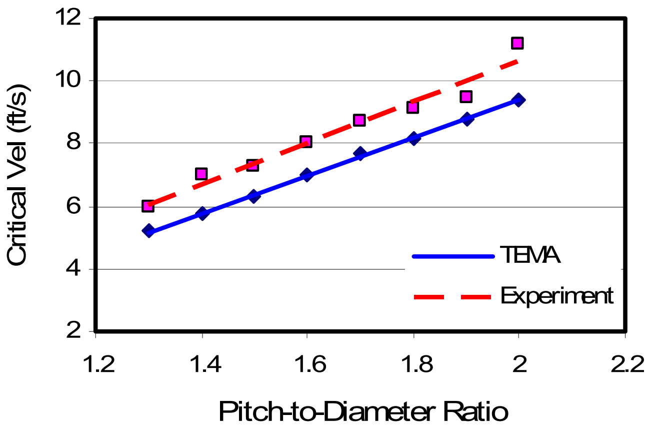

Figure 8: Critical velocity estimates for rotated square array

multi-degree-of-freedom elastodynamic behavior of each tube in the bundle. A laboratory test facility with close-loop water test channel and a complicated design of an instrumented test section with a tube bundle of 25 tubes is established. The tubes were instrumented with strain gages, and the center tube was excited by a shaker at different frequencies to study a wide range of fluidelastic effects. Two configurations of tube bundles were investigated; namely the inline-square and the rotated-square tube arrays. The functionality of the augmented test facility, where fluids, structures, electronics, and digital equipment are all interconnected, was manifested by successful measurements of the fluidelastic coefficients at a wide range of parameter variations.

The experimental results show clearly the dependency of the measured coefficients on the excitation frequency, which is an important factor that was ignored by previous investigations. The experimentally identified fluidelastic coefficients are utilized by a computer program in MATLAB code, developed in Part-I of this paper, to compute the critical velocities that define the threshold of instability for a given set of heat exchanger parameters. As pointed out in Part-I, the developed numerical scheme utilizes the finite element method, wherein the fluidelastic coupling is more accurately calculated for being treated as distributed over the entire tube length. Another important finding, which was verified in the field, is gleaned out from comparisons with TEMA guidelines. It was demonstrated that TEMA guidelines are on the conservative side for the two cases considered in this experimental investigation.

Acknowledgement

This research work is funded by Saudi Aramco, Project No. ME2212. The authors greatly appreciate the support provided by Saudi Aramco and King Fahd University of Petroleum & Minerals during this research.

References

[1] Wallis, R.P., 1939, “Photographic Study of Fluid Flow between Banks of Tubes”, Engineering, **148**, pp.423-426.

[2] Putnam, A.A., 1959, “Flow Induced Noise in Heat Exchangers*”,* J. Eng. Power, Ser. A, **81** (4), pp.417-422.

[3] Paidoussis, M. P., (1983), “A review of flow-induced vibrations in reactor and reactor components”, Nuclear Engineering and Design, **74**, pp. 31-60.

[4] Price, S. F., 1995, “A review of theoretical models for fluid-elastic instability of cylinder arrays in crossflow”, Journal of Fluids and Structures, **9**, pp. 463-518.

[5] Weaver, D. S., Ziada, S., Au-Yang, M. K., Chen, S. S., Paidoussis, M. P., and Pettigrew, M.J., 2000, “Flow-Induced Vibrations in Power and Process Plant Components-Progress and Prospects”, ASME Journal of Pressure Vessel Technology, **122**, pp. 339-348.

[6] Chen, S., 1987, *Flow-Induced Vibrations of Circular Cylindrical Structures*, Hemisphere Publishing Corp, New York, NY.

[7] Katinas, V. and Zukauskas, A., 1997, *Vibrations of Tubes in Heat Exchangers*, Begell House, Inc., NY, USA,.

[8] Chen, S.S., 1983, “Instability Mechanisms and Stability Criteria of a Group of Circular Cylinders Subjected to Cross-Flow - Part 1: Theory”, ASME Journal of Vibration, Acoustics, Stress & Reliability in Design, **105** (1), pp. 31-39.

[9] Chen, S.S., 1983, “Instability Mechanisms and Stability Criteria of a Group of Circular Cylinders Subjected to Cross-Flow - Part 2: Numerical Results and Discussions”, ASME Journal of Vibration, Acoustics, Stress & Reliability in Design, **105**, pp. 253-260.

[10] Cai, Y., Chen, S.S. and Chandra, S., 1992, “A Theory for Fluidelastic Instability of Tube-Support Plate Inactive Modes”, ASME Journal of Pressure Vessel Technology, **114**, pp. 139-148.

[11] Eisinger, F.L., Rao, M.S.M., Steininger, D.A., and Haslinger, K.H., 1995, ”Numerical Simulation of Cross-Flow-Induced Fluidelastic Results” ASME J. of Pressure Vessel Technology, **117**, pp. 31–39.

[12] Ichioka, T., Kawata, Y., Nakamura, T., Izumi, H., Kobayashi, T. and Takamatsu, H., 1997, “Research on Fluid Elastic Vibration of Cylinder Arrays by Computational Fluid Dynamics: Analysis of Two Cylinders and a Cylinder Row”, JMSE Int. Journal, Series B, **40**(1), pp. 16-24.

[13] Kassera, V. and Strohmeier, K, 1997, “Simulation of tube bundle vibrations induced by cross-flow”, J. Fluids & Structures, **11**, pp. 909-928.

[14] Fischer, M. and Strohmeier, K., 1999, “Three-Dimensional Simulation of Single Fixed-Fixed Tube Vibration Induced By Cross-Flow Including Bending and Torsion”, ASME PVP-**396**, Emerging Technologies in Fluids, Structures, and Fluid/Structure Interactions, pp. 285-290.

[15] Grover, L.K. and Weaver, D.S., 1978, “Cross-Flow Induced Vibration in a Tube Bank-Vortex Shedding”, J. Sound & Vibration, **59**, pp. 263-276.

[16] Weaver, D.S. and Grover, L.K., 1978, “Cross-Flow Induced Vibration in a Tube

Bank-Turbulent Buffeting and Fluid Elastic Instability", J. Sound & Vibration, **59**, pp.277-294.

[17] Tanaka, H. and Takahara, S., 1981, "*Fluid* Elastic Vibrations of Tube Array in Cross Flow", Sound & Vibration, **77** (1), pp.19-37.

[18] Tanaka, H., Takahara, S. and Ohta, K., 1982, "Flow-induced Vibrations in Tube Arrays with Various Pitch-to-Diameter Ratios", SME Journal of Pressure Vessel Technology, **104**, pp. 168-174.

[19] Tanaka, H., Tanaka, K., Shimiuz, F., and Takahara, S., 2002, "Fluidelastic Analysis of Tube Bundle Vibrations in Cross-flow", J. Fluids & Structures, **16**(1), pp. 93-112.

[20] Granger, S., Campistron, R., and Lebret, J., 1993, "Motion-Dependent Excitation Mechanisms in a Square In-Line Tube Bundle Subject to Wear Cross-Flow: An Experimental Modal Analysis", Journal of Fluids and Structures, **7**, pp.521-550.

[21] Chen, S.S., Zhu, S., and Jendrzejczyk, J.A., 1994, "Fluid Damping and Fluid Stiffness of a Tube in Crossflow", ASME J. of Pressure Vessel Technology, **116**, pp. 370-383.

[22] Chen, S.S., Cai Y., and Zhu, S., 1996, "Flow-Induced Vibration of Tubes in Cross-Flow", J. Offshore Mechanics & Artic Engineering, **118**, pp. 253-258.

[23] **TEMA** (Standards of Heat Exchanger Manufacturer Association), **Mechanical Standards TEMA Class RCB**, Section 5, pp.34.

[24] Perzemieniecki, 1968, *Matrix Structural Analysis*, McGraw-Hill Inc.

[25] Bazoune, A., Stephen, N.G. and Khulief, Y.A., 2003, "Shape Functions for Three-Dimensional Timoshenko Beam Elements", J. Sound & Vibration, 259 (2), pp.473-480.

[26] Khulief, Y.A., Al-Kaabi, S., Said, S., and Anis, M., "Flow-Induced Vibrations in Tubular Heat Exchangers: Part-I Numerical Model", **ASME J. Pressure Vessel Technology,** Vol.131/011301, 2009

[27] Neumaier, A., 1985, "Residual inverse iteration for the nonlinear eigenvalue problem" ,SIAM J. Numer. Anal. **22**, pp. 914-923.

[28] Conca, C., Planchard, J., and Vanninathan, M, 1989, "Existence and location of eigenvalues for fluid-solid structures", Comput. Meth. Appl. Mech. Engrg., **77**, pp. 253-291.

[29] Khulief, Y.A., Al-Kaabi, S., Said, S., and Anis, M., "Flow-Induced Vibrations in Tubular Heat Exchangers: Part-II Experimental Investigation", **ASME J. Pressure Vessel Technology,** Vol.131/011302, 2009.